Food Hydrocolloids 123 (2022) 107191

Contents lists available at ScienceDirect

Food Hydrocolloids

journal homepage: www.elsevier.com/locate/foodhyd

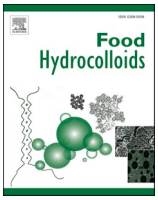

Effect of calcium enrichment on the composition, conformation, and functional properties of soy protein

Yu Peng [a], Konstantina Kyriakopoulou [a], Julia K. Keppler [a], Paul Venema [b], Atze Jan van der Goot [a,*]

[a] Food Process Engineering Group, Wageningen University, Bornse Weilanden 9, 6708, WG, Wageningen, the Netherlands
[b] Laboratory of Physics and Physical Chemistry of Foods, Wageningen University, Bornse Weilanden 9, 6708, WG, Wageningen, the Netherlands

ARTICLE INFO

Keywords:
Soybean protein
Aqueous fractionation
Simplified process
Calcium enrichment
Sodium reduction
Functional properties

ABSTRACT

Plant-based diets with sufficient calcium (Ca) supplements are needed to protect the body from Ca deficiencies. The Ca enrichment of protein ingredients during fractionation can provide a new route to increase the Ca content in plant-based products. We, therefore, investigated if the partial replacement of NaOH by $Ca(OH)_2$ during the neutralization step of the fractionation process affects the functional properties of the protein-rich fractions. The protein and oil content of the obtained soy protein-rich fractions (SPFs) were not affected by the use of $Ca(OH)_2$. Moreover, when the Ca content in the SPF was lower than a certain threshold value (6.5 mg Ca/g protein), the functional properties and conformation of SPF did not change significantly. Higher Ca content in the SPF, however, led to protein-rich fractions with larger particle size, higher thermal stability, lower NSI and WHC_P values, and weaker gel networks. Thus, any addition of Ca higher than a certain threshold changes the properties of the proteins significantly, which can alter the applicability of the fractions in plant-based food products. Nonetheless, this study showed that with partial replacement of NaOH by $Ca(OH)_2$, the enrichment of SPF with Ca is possible without strongly influencing the SPF properties.

1. Introduction

Plant-based diets aim to minimize animal foods, such as meat, dairy, and eggs (Lynch, Johnston, & Wharton, 2018; Tuso, Ismail, Ha, & Bartolotto, 2013). They have become more widespread among the population in the promotion of physical and environmental health (Rizzo & Baroni, 2018). Therefore, it is important that plant-based diets are balanced, and that they can provide all essential nutrients. Animal-based foods such as dairy products are naturally rich in calcium (Ca), while their Ca bioavailability is also high. This is because Ca is chelated in casein micelles enabling high solubility in food and intestinal lumen (Gaucheron, 2005). However, common plant sources including most vegetables, fruits, and cereal grains are lacking in Ca (Keller, Lanou, & Barnard, 2002). Additionally, protein-rich sources like dried beans have substantially lower Ca bioavailability because of the presence of phytate, which can inhibit Ca absorption (Weaver, Heaney, Proulx, Hinders, & Packard, 1993). This poses a hurdle specifically for vegans to reach the recommended dietary Ca intake of 1000 mg per day (Institute of Medicine (US), 2011). Early studies showed that vegans have a considerably lower average Ca intake than recommended levels compared to vegetarians and omnivores (Davey et al., 2003; Larsson & Johansson, 2002). This low Ca intake increases the risk of bone fracture and osteoporosis because Ca is essential for bone health (Appleby, Roddam, Allen, & Key, 2007; Wójcik et al., 2020). Thus, it is advisable for individuals who choose a plant-based diet and limit dairy products to include Ca-enriched foods or supplements.

Among plant-based diets, soy and soy foods have attracted industrial interest due to their high nutrient content and versatile properties (Hoffman & Falvo, 2004). Soybeans are rich in phytate, but the Ca-enriched soy-foods such as Ca-fortified soy milk (1000 mg Ca/L) and Ca-set tofu (117 mg Ca/100g) have been proven to be good sources of bioavailable Ca for humans (Weaver et al., 2002; Y. Zhao, Martin, & Weaver, 2005). Different soluble and less-soluble calcium salts can be used for Ca enrichment of soy protein, such as calcium chloride, calcium carbonate, calcium phosphate, calcium citrate, and calcium gluconate. The use of certain salts however may lead to changes in the physico-chemical properties of protein as well as the Ca bioavailability (Acosta et al., 2020). Moreover, Ca enrichment can be done in different steps

* Corresponding author.
E-mail address: atzejan.vandergoot@wur.nl (A.J. van der Goot).

https://doi.org/10.1016/j.foodhyd.2021.107191
Received 22 May 2021; Received in revised form 11 September 2021; Accepted 14 September 2021
Available online 17 September 2021

throughout the process chain of soy foods. For example, $CaSO_4$ is used as a coagulant for tofu production (Rekha & Vijayalakshmi, 2013), while Ca fortifiers are often added after the soy milk preparation (Z.-G. Li, Yue, Liu, & Zhang, 2011; Yazici, Alvarez, Mangino, & Hansen, 1997). $CaCl_2$ has been used for the Ca enrichment of commercially available soy ingredients such as soy protein isolate (SPI) (Manassero, Vaudagna, Añón, & Speroni, 2015; Piccini, Scilingo, & Speroni, 2019), which is a popular ingredient for novel soy-foods such as meat and dairy analogues (Baldassarre et al., 2020; Bhatia & Greer, 2008).

To obtain soy protein-rich ingredients from soybeans or de-fatted soy meals, an aqueous fractionation with alkaline solubilization and isoelectric precipitation steps can be used to achieve high protein purity. NaOH is commonly used for the pH adjustments during the fractionation, which introduces a certain amount of Na to the ingredients (Nicolas A. Deak & Johnson, 2007). In the human diet, extra Na intake can raise blood pressure, which increases the risk of cardiovascular disease (Strazzullo, D'Elia, Kandala, & Cappuccio, 2009). It might also enhance urinary Ca losses, leading to the opposite effect of our initial purpose (Itoh & Suyama, 1996; Matkovic et al., 1995; Mitchell, 2019). Therefore, we see the need for a new route to enrich the Ca and reduce the Na content broadly for novel soy-foods.

Several attempts have been made to enrich the Ca content in SPI. For example, Manassero et al. re-dispersed the SPI powder into water, and added the $CaCl_2$ in the dispersions afterward (Manassero et al., 2015); Piccini et al. fractionated the SPI first and added $CaCl_2$ before or after denaturing treatments (Piccini et al., 2019). These types of Ca enrichment occurred after the protein separation stage, so the post-processing steps are needed, and the NaOH has already been introduced for the pH adjustments during the fractionation process. In our previous work, we used a simplified aqueous fractionation, in which the de-fatting and washing steps were omitted. The $Ca(OH)_2$ was explored as an alternative to NaOH in the alkaline solubilization and neutralization step. This strategy was found beneficial in providing higher Ca content and lowering Na content in soy ingredients. It was concluded that replacing NaOH with $Ca(OH)_2$ in the solubilization step increased protein recovery, while the replacement in the neutralization step achieved high-Ca low-Na fractions (Peng, Dewi, Kyriakopoulou, & van der Goot, 2020, p. 102501). However, both Na and Ca ions can screen electrostatic interactions between charged protein molecules, whereas divalent salt ions like Ca ions also have the ability to cross-link negatively charged carboxylic acid groups on neighboring protein molecules (Hongsprabhas & Barbut, 1997). Thus, the added effect from the formation of salt bridges altered the functionalities of proteins. Our previous study reported that a complete replacement of NaOH with $Ca(OH)_2$ greatly varied the protein solubility, which could bring challenges for further applying the ingredients in soy-based products.

We hypothesize that there is a critical Ca concentration upon which the soy protein functionalities are affected. Thus, the present study investigates a step-wise increase of $Ca(OH)_2$ in the neutralization step by mixing NaOH and $Ca(OH)_2$ in different ratios in a simplified fractionation process. The obtained soy protein-rich fractions (SPFs) are examined with respect to composition, protein conformation (FTIR), charge density (zeta-potential), morphology (SEM), aggregate size, nativity (DSC), and relevant functionalities such as protein solubility, water holding capacity, and gelling properties. The results also provide more insights into how Ca ions bind to soy. With those experiments, we aim to create soy protein ingredients with enriched Ca content, as well as the desired range of functionalities for developing novel soy-based products.

2. Materials and methods

2.1. Materials

Dry, full soybeans (with hulls) were obtained from FRANK Food Products (Twello, The Netherlands) and stored in a cooling room (4 °C). Analytical grade NaOH, $Ca(OH)_2$, and HCl were purchased from Sigma-Aldrich (St. Louis, Missouri, U.S.A). Ultrapure water from a Milli-Q Lab Water System (Milli-Q IQ 7000 Ultrapure Lab Water System, Merck KGaA, Darmstadt, Germany) was used throughout the study unless stated otherwise.

2.2. Methods

2.2.1. Full-fat soy flour (FFSF) preparation

Full-fat soy flour was prepared according to the methods developed earlier (Peng, Kersten, Kyriakopoulou, & van der Goot, 2020, p. 102501). In short, full soybeans (with hulls) were pre-milled to soy grits, and the soy grits were further milled into FFSF. Around 5 kg of FFSF were produced and stored in a cooling room (4 °C) for further analysis and processing. The FFSF contained 38.9% ± 4.2% of protein and 20.6% ± 0.6% of oil on a dry basis.

2.2.2. Soy protein-rich fractions preparation

Soy protein-rich fractions (SPFs) were fractionated based on the process developed earlier (Peng, Dewi, et al., 2020, p. 102501). An overview of the processing steps and parameters can be found in Fig. 1. Briefly, FFSF was mixed with 30 mM NaOH to achieve a dispersion with a pH between 8 and 9 (alkaline solubilization step), which was subsequently centrifuged at 20,000×*g* for 30 min (25 °C). After centrifugation, the protein-rich supernatant was collected, and the pH of the supernatant was adjusted between 4.5 and 5 by adding 1 M HCl (acid precipitation step). The dispersion was stirred for 1 h and centrifuged as above. The protein-rich pellet was neutralized to pH 6.5–7 with a NaOH and $Ca(OH)_2$ mixture (protein neutralization step). All the mixtures were prepared in advance with a fixed OH^- concentration of 30 mM, which was achieved through applying combinations of NaOH and $Ca(OH)_2$ solutions (Table 1). The pH of the mixtures was between 12.4 and 12.5. The NaOH and $Ca(OH)_2$ concentrations were selected based on the solubility limitation of $Ca(OH)_2$ and preliminary experiments.

After the protein neutralization step, the protein-rich dispersions were freeze-dried (Freeze Dryer, Martin Christ, Osterode, Germany). The dried materials were milled into powders and stored in a cooling room (4 °C) until further analysis. All samples were prepared in duplicate.

2.2.3. Composition analysis

The protein content of FFSF and SPFs was determined by using Dumas analysis (Rapid N exceed, N/Protein Analyzer, Elementar, Germany) with a conversion factor of 5.7 (Krul, 2019). The oil content was measured using the Buchi extraction system (Buchi Labortechnik AG, Flawil, Switzerland) with petroleum ether as the extraction solvent. The Ca and Na contents in the SPFs were determined by a standard procedure using inductively coupled plasma optical emission spectrometry (AVIO 500, PerkinElmer, Waltham, MA). A multi-element standard (Merck P/N 1.11355) was used, and the results are expressed as the total concentration of Ca and Na ions compared with the standard sample.

2.2.4. Powder morphology analysis

The morphology of all the SPF powders was determined by scanning electron microscopy (SEM) (JCM-7000 NeoScope™ Benchtop SEM, JEOL Ltd., Japan). The protein powder was placed evenly on an aluminium sample holder using double-sided adhesive conductive carbon tape, and the powder morphology was observed with an accelerating voltage at 5 kV.

2.2.5. Particle size analysis

The particle size distribution (PSD) of the SPFs was measured with a laser light scattering instrument (Mastersizer 3000, Malvern Instruments Ltd, United Kingdom) and a wet module (Hydro SM, Malvern Instruments Ltd, United Kingdom). For these measurements, 1% (w/v) SPF dispersions were prepared with Milli-Q water. A refractive index of 1.45 was used for the dispersion phase and 1.33 for the water continuous

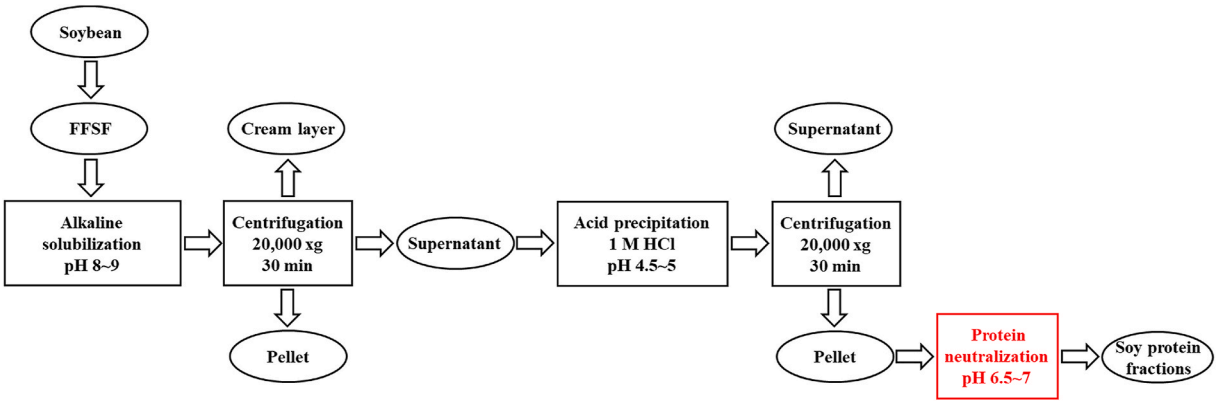

Fig. 1. Simplified fractionation process to produce soy protein-rich fractions (SPFs).

Table 1
Concentrations of NaOH and $Ca(OH)_2$ for preparing the alkaline mixtures used at the protein neutralization step to investigate a step-wise increase of the Ca content in the different SPFs.

Sample name	NaOH concentration [mM]	$Ca(OH)_2$ concentration [mM]	Total OH^- concentration [mM]	pH
SPF 1	30	0	30	12.48
SPF 2	25	2.5	30	12.44
SPF 3	20	5	30	12.43
SPF 4	15	7.5	30	12.44
SPF 5	10	10	30	12.43
SPF 6	5	12.5	30	12.41
SPF 7	0	15	30	12.41

phase.

2.2.6. FT-IR analysis

The effect of Ca or Na on the conformation of the SPFs was analysed using a Confocheck™ Invenio-S Fourier Transform Infrared (FT-IR) spectrometer equipped with a temperature-controlled Bio ATR2 unit and a MCT detector (Bruker Optics, CITY, Netherlands) optimized for protein analytics in solutions as previously described by Kayser et al. (Kayser, Arnold, Steffen-Heins, Schwarz, & Keppler, 2020). 1% (w/v) SPF dispersions (neutral pH) were prepared, and the measurements were conducted at a temperature of 25 °C against the respective solvent mixtures without protein as background and averaged over 120 scans at a resolution of 0.7 cm. The second derivative of the amide I band (1590-1700 cm^{-1}) was calculated using nine smoothing points.

2.2.7. Zeta potential analysis

The charge density of the SPFs at different pHs was determined with a dynamic light scattering apparatus (Zetasizer Nano ZS, Malvern Instruments Ltd, United Kingdom). A disposable cuvette (Folded Capillary Zeta Cell DTS1070, Malvern Instruments Ltd, United Kingdom) was filled with a 1% (w/w) SPF dispersion. Titration was performed (MPT-2 autotitrator, Malvern Instruments Ltd, United Kingdom) to adjust the pH of the dispersions from 3 to 9 in steps of 0.5 either with a HCl (0.25 M) or a NaOH (0.25 M). The refractive indices used were 1.43 for the dispersed phase and 1.33 for the continuous phase.

2.2.8. Protein solubility analysis

The nitrogen solubility index (NSI) was used to evaluate protein solubility at pH 3 and pH 7. A 2% (w/w) dispersion of each SPF sample was placed in a centrifuge tube and rotated overnight. After that, the pH of the dispersions was adjusted by adding 1 M HCl and checked every half an hour. Once the pH value became constant (pH 3 or pH 7), the dispersions were centrifuged at 20,000×*g* for 30 min to separate the supernatant and pellet. The nitrogen content was measured by using Dumas analysis (Rapid N exceed, N/Protein Analyzer, Elementar, Germany), and the NSI was calculated by the ratio of soluble nitrogen over the total initial nitrogen content present in the SPFs.

2.2.9. Denaturation behaviour analysis

The denaturation behaviour of the SPFs was determined by differential scanning calorimetry (Diamond DSC, PerkinElmer, USA). A 20% (w/w) protein dispersion of each powder was prepared in a high-volume aluminium pan, which was then well sealed. The DSC analysis was carried out in two steps: heating from 20 °C to 150 °C with a gradient of 5 °C/min, and subsequent cooling step from 150 to 20 °C with a gradient of 10 °C/min. An empty high-volume aluminium pan was used as a reference. The denaturation temperature (T_d) and enthalpy of transition were determined from the DSC graph by Start Pyris Software (PerkinElmer, USA), and the denaturation temperature was defined as the temperature at which a maximum occurred in the endothermic peaks.

2.2.10. Water holding capacity

The water holding capacity (WHC) of the SPFs was determined by using the method described by Peters (Peters, Vergeldt, Boom, & van der Goot, 2017) with slight modification. SPF sample (M_1) was placed in a centrifuge tube with water to make a 2% (w/v) SPF dispersion and rotated overnight. Then, the dispersion was centrifuged at 20,000×*g* for 30 min (25 °C). The supernatant was discarded, and the wet pellet was collected and weighed (M_2). Subsequently, the wet pellet was oven-dried overnight at 105 °C and weighed again to determine the mass of the dry pellet (M_3). The WHC was calculated according to Equation (1) and the WHC of the pellet (WHC_P) was calculated according to Equation (2).

$$WHC\ \left(\frac{g\ water}{g\ dry\ SPF\ powder}\right) = \frac{M_2 - M_3}{M_1} \quad (1)$$

$$WHC_P\ \left(\frac{g\ water}{g\ dried\ pellet}\right) = \frac{M_2 - M_3}{M_3} \quad (2)$$

2.2.11. Viscosity analysis

SPF dispersions standardized on 9 wt% protein (approximately 12 wt % SPF) were prepared and stirred for around 1 h. A stress-controlled rheometer (Anton Paar Physica MCR 301, Graz, Austria) combined with a sand-blasted CC-17 concentric cylinder geometry was used to determine the viscosity. The SPF dispersion was equilibrated for 5 min, and a shear rate sweep was performed at 25 °C from 0.1 to 100 s^{-1}.

2.2.12. Gelation behaviour analysis

A stress-controlled rheometer (Anton Paar Physica MCR 301, Graz, Austria) combined with a sand-blasted CC-17 concentric cylinder geometry was used. SPF dispersions standardized on 9 wt% protein

concentration (approximately 12 wt% SPF) were prepared and stirred for 1 h before the measurements. A thin layer of high-temperature-resistant silicone oil was covered on top of the samples to prevent water evaporation during heating. A temperature, frequency, and strain sweep were performed sequentially. The temperature sweep was done by increasing the temperature from 20 to 95 °C at a rate of 3 °C/min, followed by 10 min at 95 °C before cooling back to 20 °C at a rate of 3 °C/min. The storage (G') and loss modulus (G'') were recorded as a function of time. The point where the storage and loss modulus crossed was taken as the gel point, while the temperature at that point was defined as the gelation temperature (T_{gel}) (Spotti, Tarhan, Schaffter, Corvalan, & Campanella, 2017). Subsequently, the samples were exposed to a frequency sweep from 0.01 to 10 Hz (at a strain of 1%), and a strain sweep from 0.1 to 1000% (at a frequency of 1 Hz). The storage (G') and loss modulus (G'') dependency on frequency, and strain were recorded.

2.2.13. Statistical analysis

The different fractionation schemes (with the varied neutralization conditions) were performed in duplicate, and if not stated otherwise, all data were collected for each sample from at least triplicate measurements. SPSS Statistics Version 23.0 (IBM, USA) was used to analyses the variance, and Duncan's test was performed to determine the statistical significance between samples at an α level of 0.05. All the results are displayed as mean values ± standard deviations.

3. Results

In this study, SPFs were obtained through a simplified fractionation process and neutralized by NaOH and $Ca(OH)_2$ in different ratios to identify critical ratios that affect the protein functionality. The variations in the neutralization step led to differences in the composition, particle morphology, charge density, and functional properties of the SPFs.

3.1. Composition

The protein content of all SPFs was similar and around 75% on a dry basis (Table 2). The oil content varied from 1.21% to 2.53%, which was much lower than the oil content in the start material FFSF. These results also agreed with the values reported by our previous study (Peng, Dewi, et al., 2020, p. 102501). In terms of Na and Ca content, the differences between SPFs were significant. SPF 1, for which only NaOH was used in the neutralization step, had the highest amount of Na (15.9 mg/g protein) and the lowest amount of Ca (0.6 mg/g protein). As expected, we observed a higher Ca content and lower Na content when using more $Ca(OH)_2$ to neutralize the SPF dispersions. The Ca content of SPF 7 (16.6 mg/g SPF) was around 29 times higher than that of SPF 1, while the Na content of SPF 7 (0.8 mg/g SPF) was only 5% of the level found in SPF 1. In addition, the exact Ca and Na contents measured for all SPF samples were quite close to the amount of Ca and Na added in the neutralization step during the fractionation.

Table 2
The composition of the SPFs (dry basis).

Sample name	Protein (%)	Oil (%)	Na content (mg/g protein)	Ca content (mg/g protein)
SPF 1	75.06 ± 2.17^{a}	1.52 ± 0.52^{bc}	15.91 ± 1.29^{a}	0.57 ± 0.06^{g}
SPF 2	74.53 ± 1.20^{a}	1.21 ± 0.06^{c}	11.02 ± 0.75^{b}	1.90 ± 0.12^{f}
SPF 3	74.70 ± 0.65^{a}	1.76 ± 0.26^{abc}	9.80 ± 0.05^{c}	4.28 ± 0.02^{e}
SPF 4	75.27 ± 0.75^{a}	2.07 ± 0.28^{abc}	7.47 ± 0.47^{d}	6.47 ± 0.40^{d}
SPF 5	74.34 ± 1.85^{a}	2.53 ± 0.90^{a}	5.67 ± 0.24^{e}	9.84 ± 0.41^{c}
SPF 6	75.55 ± 0.93^{a}	2.04 ± 0.70^{abc}	2.84 ± 0.09^{f}	12.62 ± 0.29^{b}
SPF 7	75.73 ± 0.28^{a}	2.18 ± 0.67^{ab}	0.81 ± 0.02^{g}	16.55 ± 0.66^{a}

*The values in the table are compared in columns and different higher case letters indicate a significant difference ($P < 0.05$).

3.2. Powder morphology

SPFs prepared with different $Ca(OH)_2$ and NaOH ratios appeared to have some differences in their microstructure (Fig. 2). SPF 1, neutralized by NaOH during the fractionation process, showed a lamellar glass-like structure with a smooth clean surface (red arrow). Although no major differences were observed between SPF 1 and SPF 2, while increasing the Ca content (SPF 4 and SPF 5), a rougher flake surface was observed (blue circle) next to the glassy structure. At the highest Ca content of SPF 6 and SPF 7, the lamellar structures largely disappeared and a pumice stone structure with a rough sponge-like surface emerged.

3.3. Particle size distribution (PSD)

The PSD curves of 1% SPF dispersions in water (Fig. 3) showed a gradual shift to the right with the increase of the Ca content in the SPFs from SPF 1 to SPF 7. The distributions of SPF 1 and SPF 2 were quite similar with a single peak around 48 μm and 55 μm, respectively. For SPF 3 and SPF 4, the PSD became wider towards the right side, while SPF 4 had two peak values around 38 μm and 92 μm. The rest of the curves were single-peaked, while for SPF 6 and SPF 7, a relatively narrow distribution of larger size was observed.

3.4. Secondary structure

Fig. 4 shows the mean second derivative FTIR spectra in the amide I region of the SPFs. The bands corresponding to intramolecular β-sheets were obtained in the frequency region of 1635–1640 cm^{-1} and 1670-1690 cm^{-1}, while a band for α-helix appeared in the frequency around 1650-1660 cm^{-1}. The random coil structure had a band close to 1645 cm^{-1} (Cobb, Zai-Rose, Correia, & Janorkar, 2020; Kong & Yu, 2007). Early studies suggested that 7S soy protein consists mainly of α-helix and antiparallel β-sheet structures (Nagano, Mori, & Nishinari, 1994), while the major secondary structures of 11S soy protein are β-sheet, followed by β-turn, α-helix, and random coil (Long et al., 2015). In contrast, Zhao et al. described similar conformation for 7S and 11 S, with approximately 46.7% β-sheet structures in aqueous solution (X. Zhao, Chen, Xue, & Lee, 2008). Here, the strong band at ~1635 cm^{-1} confirms a predominant β-sheet conformation of all fractions.

With the variations of Ca and Na content, some minor structural changes were observed between SPFs. The bands that corresponded to the α-helix signal at 1656 cm^{-1} were continuously decreasing with increasing the Ca content. There is a minor increase of the 1619 cm^{-1} waveband, which is indicative for intermolecular β-sheets and thus for protein aggregation for SFP 5, 6, and 7. All other structural elements were randomly changing with increasing Ca content, and thus within the natural deviation or repeated measurements.

3.5. Net charge

The zeta potential is related to the net charge residing on the surface or near-surface of a suspended particle (Song, Zhou, Fu, Chen, & Wu, 2013), and is affected by many factors such as pH, ionic strength, and temperature (Malhotra & Coupland, 2004). The measured zeta potential of the SPF dispersions changed from positive to negative values when increasing pH from 3 to 9 (Fig. 5). All samples had a neutral charge around pH 5, suggesting a similar isoelectric point (pI) and thus no influence by the exact calcium and sodium content. When the pH was further increased from 5 to 9, the zeta potential of all the SPFs became

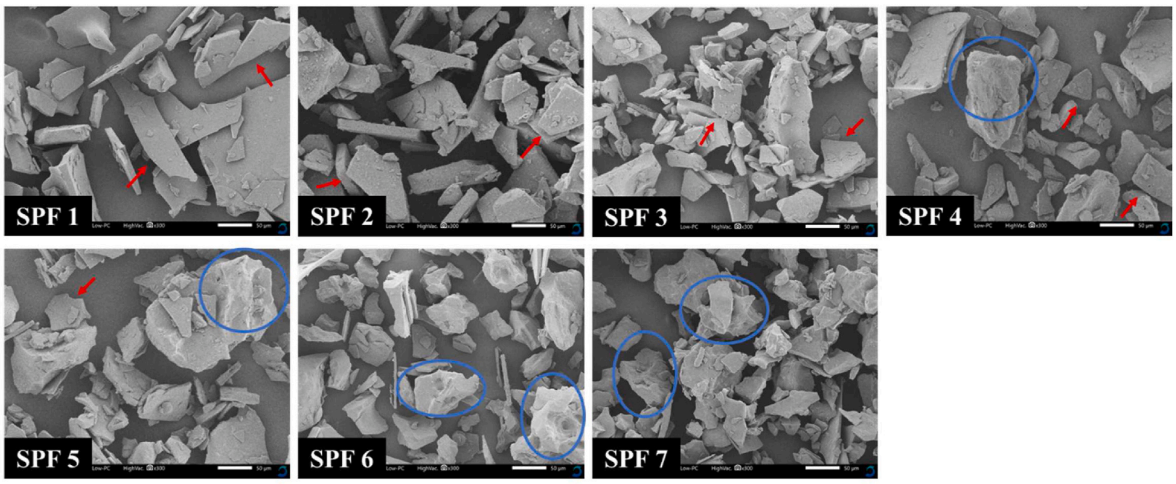

Fig. 2. Representative SEM images of the SPFs. The scale bar is 50 μm. The red arrows indicate glass-like structures with smooth surfaces, the blue circles emphasize rough surface structures. The reader is referred to the online version of the article for color presentation. (For interpretation of the references to color in this figure legend, the reader is referred to the Web version of this article.)

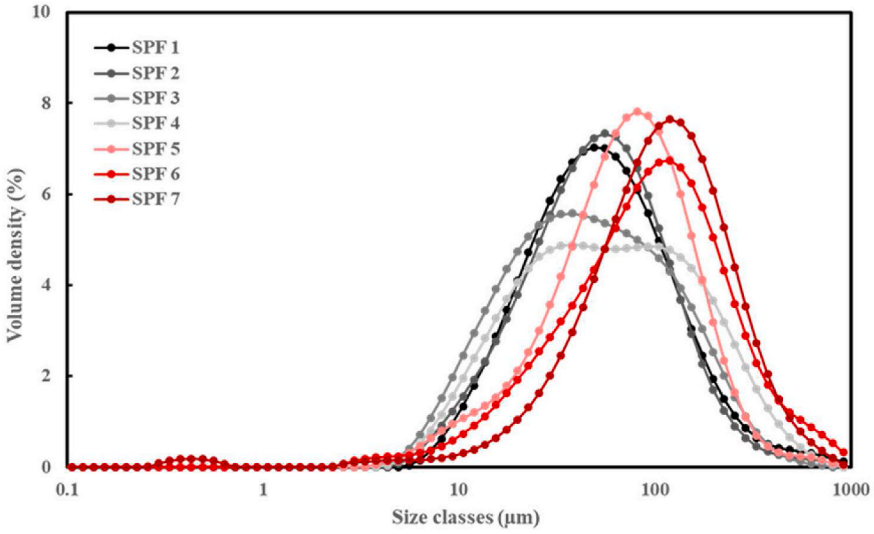

Fig. 3. Particle size distribution of 1% (w/v) SPF dispersions.

negative. In this pH range, the curves began to diverge and the differences between SPFs became visible. SPF 1 acquired the most negative charges as compared to other SPFs, while SPF 7 acquired the least amount.

3.6. Nitrogen solubility index (NSI)

The degree of protein solubility is usually represented by the nitrogen solubility index (NSI). The NSI of all the SPFs was measured at pH 3 and pH 7. When the pH was 7, the NSI decreased with higher Ca content in the SPF. SPF 1 showed a NSI of around 88.8% while the NSI-value for SPF 7 was only 10.3%. The greatest reduction in NSI happened between SPF 4 and SPF 5 where the NSI decreased from 56.9% to 26.9%. At pH 3, a higher Ca content had a similar effect on the NSI, but the NSI variation was smaller, with values ranging between 57.1% and 86.0%. The NSI measured at pH 3 was generally higher than the NSI obtained at pH 7, and the difference becoming larger with the increase of Ca content in the SPF.

3.7. Denaturation behaviours (DSC)

Two typical endothermic peaks were observed in all the SPFs, corresponding to the denaturation of β-conglycinin (7S) and glycinin (11S) (Table 3). It was observed that the T_d of 7S and 11S was influenced by the Ca levels in the SPFs. Up to 6.47 mg/g protein, the increase of Ca content hardly altered the T_d of 7S, while an increase from 75.50 to 81.97 °C was found once the Ca content was higher than that value. In contrast, the T_d of 11S increased already upon an increase of Ca content from 0.57 to 1.90 mg/g protein, which means that Ca influenced the T_d of 11S more than the T_d of 7S. These results are in agreement with previously reported results, which showed that no changes in T_d of 7S were found when lower Ca content was added in SPI dispersions, while higher T_d of 11S was found with the presence of Ca (Scilingo & Añón, 1996). The enthalpies corresponding to the denaturation of 7S and 11S proteins are shown in Table 3. The increase in Ca content in SPFs was accompanied by an increase in the enthalpy of 11S, while this effect was not significant for 7S. Overall, higher Ca content increased the thermal stability of SPF.

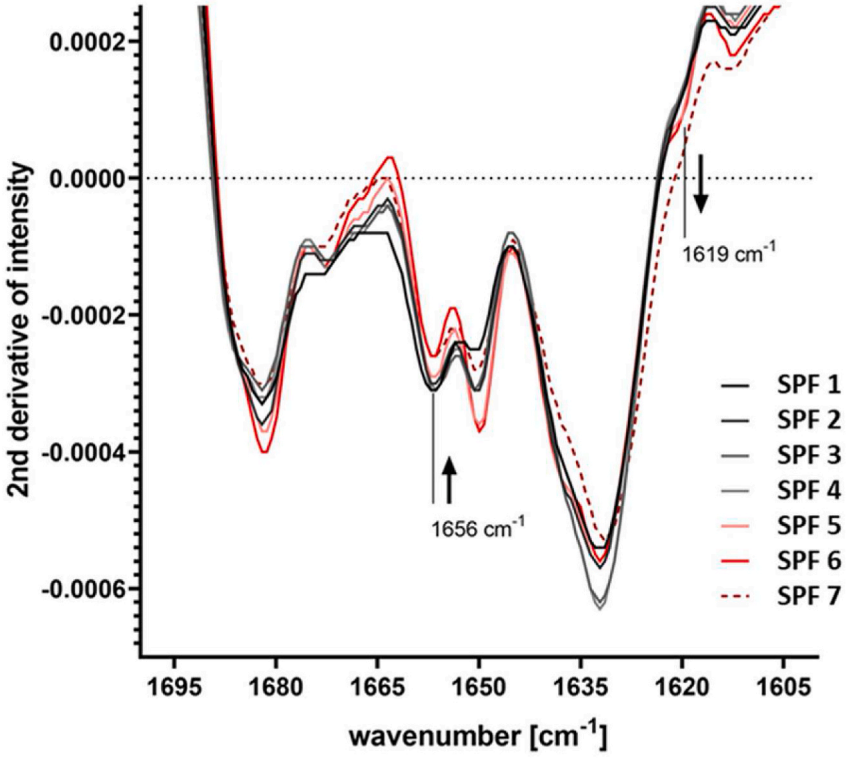

Fig. 4. Deconvoluted second derivative FTIR spectra of SPF samples (mean of three individual measurements). The arrows indicate structural elements where the intensity increases or decreases continuously with increasing Ca content.

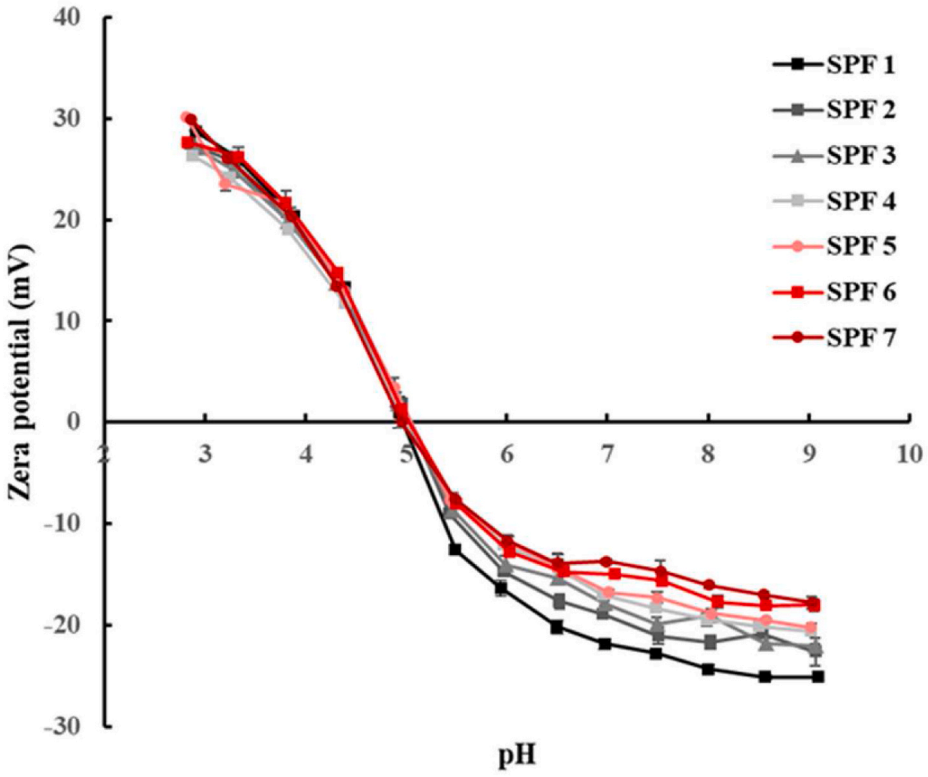

Fig. 5. Zeta potential of all the SPF dispersions as related to the pH.

3.8. Water holding capacity (WHC)

The ability to hold water is an important functionality for protein-rich ingredients, while various definitions and terms of WHC can be found in the literatures (Kneifel, Paquin, Abert, & Richard, 1991; Zayas, 1997). WHC is defined as the amount of water bound per gram of dry

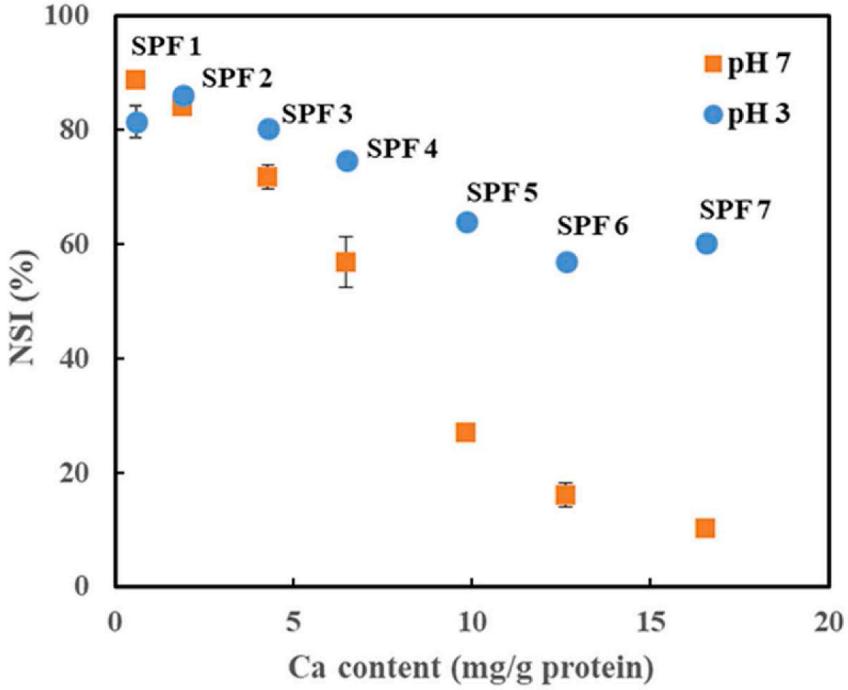

Fig. 6. Nitrogen solubility index (NSI) of all the SPFs as related to the calcium content.

Table 3
The denaturation temperature, enthalpy of the transition and gelation temperature of the SPFs.

Sample name	Ca content (mg/g protein)	7S T_d (°C)	Enthalpy (J/g)	11S T_d (°C)	Enthalpy (J/g)	T_{gel} (°C)
SPF 1	0.57 ± 0.06^{g}	75.22 ± 0.32^{d}	1.64 ± 0.20^{a}	92.76 ± 0.30^{e}	2.45 ± 0.18^{bc}	64.54 ± 2.59^{d}
SPF 2	1.90 ± 0.12^{f}	75.55 ± 0.56^{d}	1.39 ± 0.20^{abc}	94.20 ± 1.09^{d}	2.27 ± 0.07^{c}	91.87 ± 0.52^{b}
SPF 3	4.28 ± 0.02^{e}	74.71 ± 0.70^{d}	1.31 ± 0.16^{bc}	94.94 ± 1.37^{d}	2.16 ± 0.19^{c}	94.93 ± 0.54^{a}
SPF 4	6.47 ± 0.40^{d}	75.50 ± 0.41^{d}	1.22 ± 0.11^{bc}	96.53 ± 0.32^{c}	2.68 ± 0.35^{bc}	80.33 ± 5.10^{c}
SPF 5	9.84 ± 0.41^{c}	77.35 ± 0.44^{c}	1.16 ± 0.14^{c}	98.54 ± 0.54^{b}	2.84 ± 0.19^{bc}	40.22 ± 1.58^{e}
SPF 6	12.62 ± 0.29^{b}	79.56 ± 0.28^{b}	1.47 ± 0.24^{ab}	100.25 ± 0.25^{a}	3.06 ± 0.23^{b}	\
SPF 7	16.55 ± 0.66^{a}	81.97 ± 0.99^{a}	1.46 ± 0.22^{abc}	101.13 ± 0.71^{a}	3.88 ± 1.04^{a}	\

*The values in the table are compared in columns and different higher case letters indicate a significant difference ($P < 0.05$).

matter, here SPF on a dry basis. Fig. 7 shows that the WHC of all the SPFs is in the range of 1.30–3.90 g water/g SPF, and the peak value occurs at SPF 4 which contains around 6.47 mg Ca/g protein. In general, the WHC of all the SPFs was lower than the reported WHC of commercial SPI, but the peak value is comparable with the WHC of commercial SPC (Geerts, Dekkers, van der Padt, & van der Goot, 2018). The lower values could be due to differences in drying. Spray drying, as applied industrially probably leads to an increased WHC, due to the heat applied to the ingredients.

Previous research suggested that the water bound by the insoluble pellet is not necessarily a measure of water bound by the protein particles (Peters, Luyten, Alting, Boom, & Van der Goot, 2015), therefore, the WHC_P is introduced to represent the amount of water bound per gram of insoluble pellet and thus accounts for the effect of solubility on WHC (Peters et al., 2017). As the soluble part of the protein does not contribute to the WHC_P, the protein ingredients with lower NSI could potentially have more insoluble components which can hold water. However, a sharp decline of WHC_P with the increase of Ca content in the SPFs was observed, which was similar to the trend of NSI. In other words, SPF 7 showed the lowest protein solubility under pH 7 as compared to other SPFs, while it also had the lowest value of WHC_P, which means the majority of the protein in the SPF 7 is not soluble and has the weakest ability to interact with water.

3.9. Viscosity

All the SPF samples were prepared with 9 wt% protein concentration (around 12 wt% dry matter), and the flow curves are presented in Fig. 8. SPF 2 and SPF 3 presented the highest viscosity with a similar trend: a slight increase at very low shear rates suggesting shear-thickening, followed by a shear thinning behaviour. The viscosities of SPF 1 and SPF 4 were similar, while the shear thinning behaviour was also observed once the shear rate was higher than 1 s^{-1}. As for the SPF 5, SPF 6, and SPF 7, data points with torque values at or below the manufacturer reported sensitivity was omitted, and the viscosity measured at high shear rates was in the range of 0.001–0.01 Pa s, almost approaching the reported dynamic viscosity of water (0.89 mPa s, 25 °C) (https://wiki.anton-paar.com/nl-en/water/).

3.10. Gelation behaviours

The gelation behaviours of all the SPFs upon and after heating treatment were measured and are shown in Fig. 9. The left panels present the results of the temperature sweeps, in which two types of curves were observed with an increase in temperature from 20 to 95 °C. For SPF 1, SPF 2, SPF 3, and SPF 4, a decrease of G' and G'' occurred first, followed by a steep increase. However, for SPF 5, SPF 6, and SPF 7, the

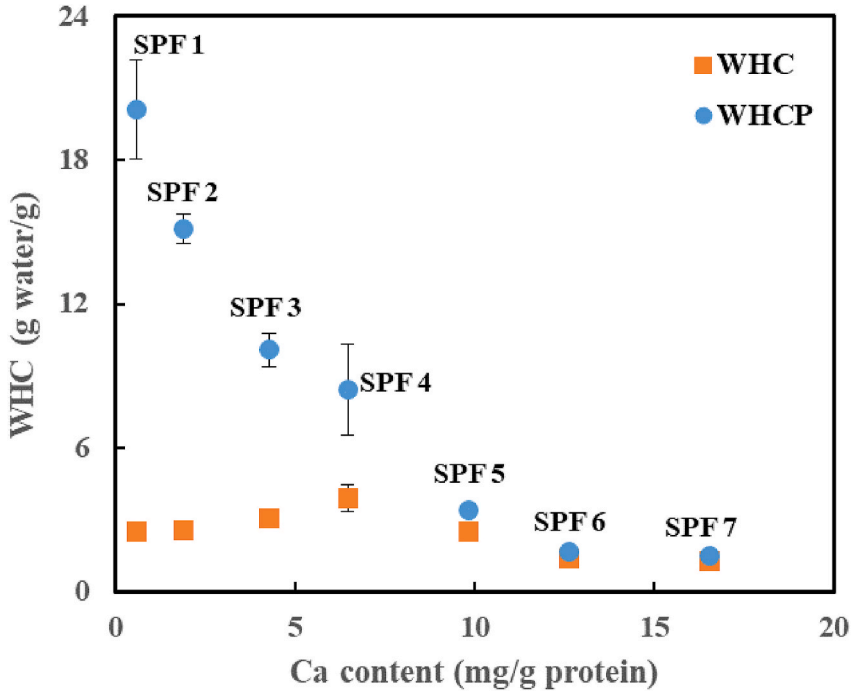

Fig. 7. Water holding capacity (WHC) and water holding capacity of the pellet (WHC_P) of all the SPFs as related to the calcium content.

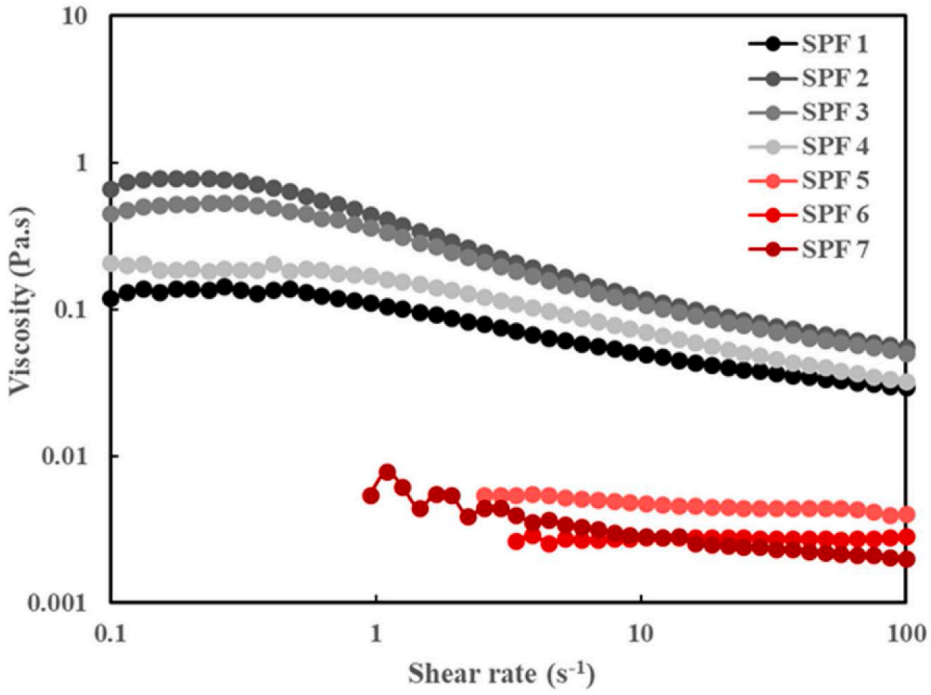

Fig. 8. Viscosity curves of the SPFs (9 wt% protein concentration) as related to the shear rate.

curve began with an increase of *G'* and *G"*, followed by a slight decrease and a sharp increase afterward.

From SPF 1 to SPF 5, the *G′* was initially lower than *G″*, so the gelation temperature (T_{gel}) for these SPFs can be detected as the cross-over temperature where the *G′* exceeds *G"* (Table 3). The T_{gel} of SPF 1 was around 64.54 °C, while the highest T_{gel} value was observed for SPF 4, which was approximately 94.93 °C. By contrast, the *G′* of SPF 6 and SPF 7 was constantly higher than *G"*, indicating that a solid-like structure was formed before heating already. In addition, a phase separation was observed with a sludge layer at the bottom and a watery layer above, this could be a result of the low solubility of SPF 6 and SPF 7, leading the sedimentation over time during the measurement. Therefore, T_{gel} was not reported in Table 3. For SPF 5 which also had a NSI lower than 30%, a cross point of G′ and G″ was observed after around 6 min of heating, which is an indication of gel formation at 40.22 °C. A thin watery layer was observed after the measurement, but it was less obvious than the layers presented above SPF 6 and SPF 7. One possible explanation could be that the fast gel formation of SPF 5 did not allow the sedimentation to take place. Besides, upon cooling, the gel firmness for all the SPFs increased.

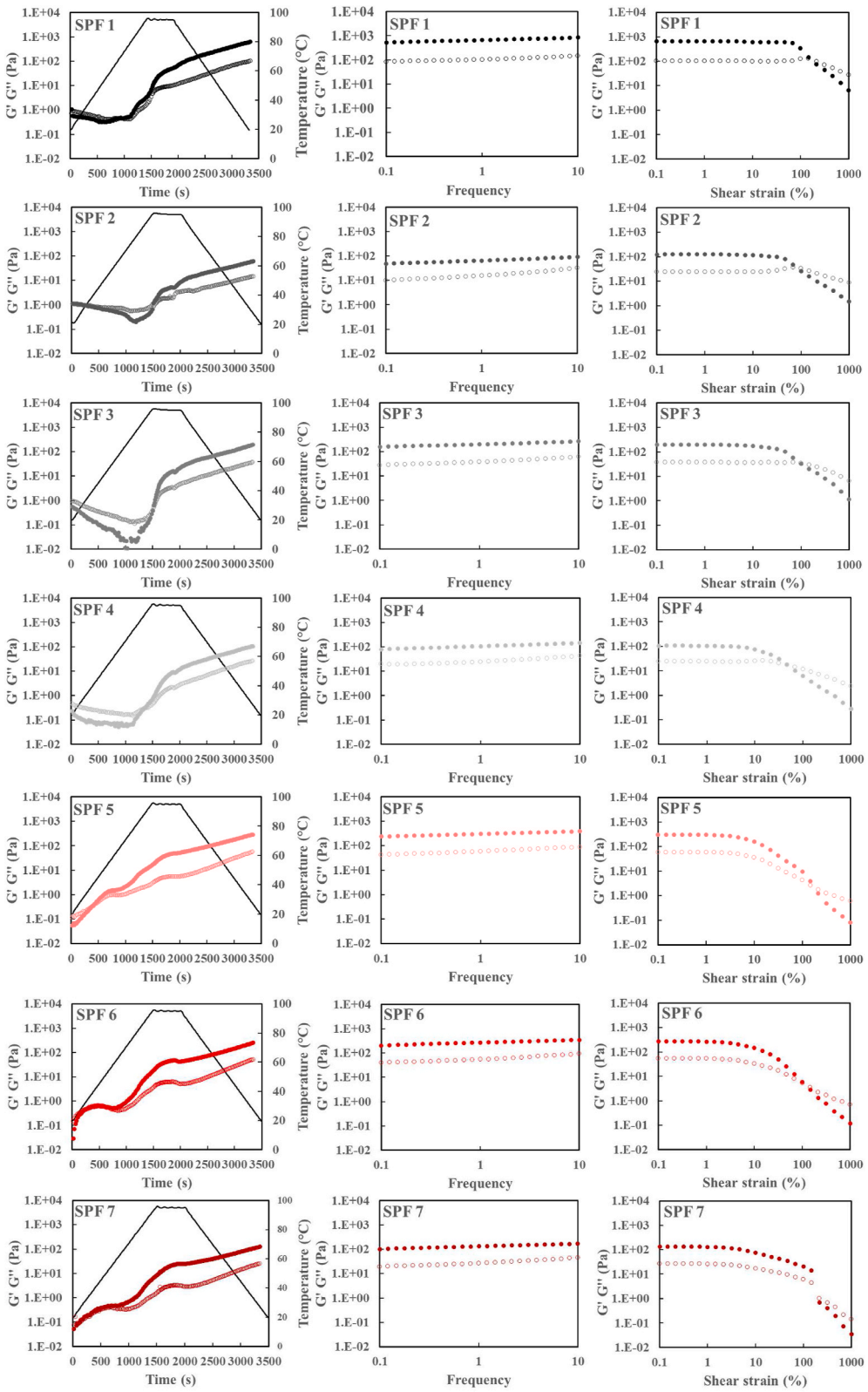

Fig. 9. Temperature (1st column), frequency (2nd column), and strain sweep (3rd column) sequentially applied on all the SPFs (9 wt% protein concentration). G': closed symbols, G": open symbols.

The G' and G'' related to the frequency were examined through a frequency sweep in a range of 0.1–10 Hz (middle panels). For all the SPFs, the G' and G'' remained generally steady over this frequency range. After frequency sweep, the length of the linear viscoelastic (LVE) regime was determined by a strain sweep in the range of 0.1–1000% with a constant frequency of 1 Hz (right panels). It was found that with the increase of the Ca content in the SPF, the LVE regime of the corresponded gel became shorter. In other words, SPF 1 has the longest LVE regime, whereas SPF 7 has the smallest maximum linear strain. These results indicate that the gel network structure of SPF 7 can be easily

disrupted as compared to other SPFs, while SPF 1 gave the strongest gel.

4. Discussions

In this study, SPFs were obtained through a simplified fractionation process and neutralized by different amounts of NaOH and $Ca(OH)_2$ during the process. Since the neutralization step was performed after the protein extraction stage, the protein and oil content of all the SPFs were quite similar (Table 2). The Ca and Na content in the SPFs varied based on the ratio of $Ca(OH)_2$ and NaOH used during the protein neutralization step (Table 1), which provides the possibility to control the Ca and Na content precisely in the ingredients during the fractionation process. From SPF 1 to SPF 7, the Ca content in the SPF gradually increased from 0.57 to 16.55 mg/g protein, while the Na content decreased from 15.91 to 0.81 mg/g protein. It is known that both Ca and Na ions can influence the electrostatic interactions, while Ca ions can also cross-link negatively-charged protein molecules forming a matrix (Mulvihill & Kinsella, 1988). Therefore, the Ca content may be more profound than Na in affecting the morphology, charge density, and functionalities of the SPFs. Hence, the following discussions mainly focused on the influences lead by the Ca content.

The powder morphology of the SPF changed from lamellar glass-like structure to pumice stone structure when higher Ca content presented in the SPF (Fig. 2). These findings were in line with the previously reported observations, in which freeze-dried SPI had a sheet-like flaky structure (Hu et al., 2013), while Ca-fortified SPI showed well defined honeycomb-like network with a certain regularity (Lee & Rha, 1978; Zhang, Liang, Tian, Chen, & Subirade, 2012). When the Ca concentration increased, the structure of soy protein became more porous and compact, and the surface was not as smooth as that obtained with lower Ca concentration (Kao, Su, & Lee, 2003). This change may be related to the formation of larger aggregates during the neutralization step. With the increase of the Ca concentration, the Ca bridges progressively became dominating, which could result in the protein aggregation into large and dense aggregates surrounded by the aqueous medium (Mulvihill & Kinsella, 1988). During freeze drying, noncontinuous structures formed, and as a result, a more porous and compact structure was observed after drying and milling steps. In contrast, at low Ca concentration, most of the proteins were highly solubilized in the dispersions after the neutralization step. In that case, a continuous structure was shaped during freeze drying, and a glass-like structure was observed after milling.

FT-IR is a powerful technique used to analyze the secondary structure of proteins. Early studies reported that native SPI showed strong absorptions at 1692, 1678, 1630 and 1619 cm^{-1}, indicating that β-sheets dominated the secondary structures in native SPI. After thermal treatment, only minor absorptions remained, and a loss of most protein secondary structures occurred during the denaturation of SPI protein (Zhang et al., 2012). In this study, the strong band around 1635 cm^{-1} confirms a predominant β-sheet conformation of all the SPFs (Fig. 4). Also, all the SPFs are still in their native state with the present of their secondary structures. This is also confirmed by the results of DSC analysis (Table 2). The overall decreasing amount of helix elements for SPF with high Ca content observed in the FTIR reveal some minor structural rearrangements of the proteins between Na and Ca additions. Previous studies reported that an increasing concentration of Ca ions likewise decreased the α-helix band of bovine serum albumin due to the direct binding of the metal ions to the protein (Alhazmi, 2019). Besides that, we also observed an increase in the 1619 cm^{-1} region at higher Ca levels (9.8 mg/g Ca, SFP 5, and above) in the present study, which hints at protein-protein interactions probably mediated by cross-linking with the bivalent metal ion (Alhazmi, 2019). Stronger protein-protein interactions are also consistent with the increasing particle size of SPF 5 to SPF 7 observed with static light scattering (Fig. 3). The 7S and 11S soy proteins each may have a different affinity for Ca binding and precipitation. Previous research found that the 11S fraction of soybean protein can be preferentially precipitated with Ca ions prior to 7S (Mitsuda, Kusano, & Hasegawa, 1965), and the binding of Ca ions is highly dependent on the pH (Appurao, A. G., 1975). It was evidenced that there are two types of binding sites for Ca ions on the protein molecules: the imidazole group, and the side-chain carboxyl groups of the aspartic and glutamic acid residues. 11S exhibits a higher affinity with a larger number of binding sites for the Ca ions, while 7S is a smaller protein and has a higher charge density (Kroll, 1984; Sakakibara & Noguchi, 1977). Besides, the precipitations of 7S and 11S begin after a threshold concentration of Ca ions is reached, while the number of Ca ions required to precipitate 7S was much larger than the amount needed for 11S (Yuan et al., 2002).

It is likely that the Ca content also affects the tested functional properties of the SPFs. The pI measured for all the SPFs was around pH 5 (Fig. 5), which was in line with previously reported data showing a pI of soy protein to be between 4.5 and 5 (Jaramillo, Roberts, & Coupland, 2011; Preece, Hooshyar, & Zuidam, 2017; Thrane, Paulsen, Orcutt, & Krieger, 2017). The decrease in electrostatic repulsions at the pI is a property that was used in this study to extract soy protein by isoelectric precipitation. When the pH was below the pI, the soy proteins were positively charged and likely repulse Ca or Na ions. As a result, the zeta potential variation of all the SPFs was similar and not influenced by the Ca and Na contents. By contrast, when the pH was above the pI, all the SPFs were negatively charged but varied between −18 mV (high Ca content) and −25 mV (low Ca content). Both Ca and Na ions could shield the electric charges of soy protein by physical attraction (Yuan et al., 2002), but Ca ions are divalent cations that lead to stronger attractive interactions. Thus, the SPFs with higher Ca content would gain fewer negative charges at a given pH higher than pI. This hypothesis is in agreement with earlier studies where pH values between pI to pH 7 increased soy protein-bound Ca ions, while at pH 7 and above, little change in bound Ca ions were seen (Kroll, 1984). Similarly, in the present study, the absolute value of zeta potential increased sharply from pH 5 to pH 7 for all the SPFs and approached a plateau in the range of pH 7 to 9.

Generally, all the SPFs exhibited higher NSI values at pH 3 than pH 7 except for SPF 1, which indicated that the effect of Ca content on the NSI of soy protein was highly dependent on the pH and the Ca-binding was reversible to a certain extent (Fig. 6). Therefore, the protein solubility changes caused by pH shift should be taken into consideration for further product development. Besides, SPFs with higher Ca content presented larger particle size and lower NSI at pH 7. These might be attributed to both hydrophobic and electrostatic interactions between soy protein molecules, leading to compact aggregates. The latter is further enhanced by the lower net charge that weakens electrostatic repulsion between proteins and lowers the solubility of SPFs. The greatest changes in particle size and NSI happened between SPF 4 and SPF 5, in which the Ca content increased from 6.47 to 9.84 mg/g protein. This might be caused by the precipitation of 7S. It was hypothesised that the Ca content in SPF 5 was sufficient to precipitate 7S, leading to the greatest changes in protein structure (FT-IR), particle size, and NSI. The differences in the precipitation of 7S and 11S of soy protein allow the production of 7S-rich fraction and 11S-fraction by utilizing calcium salts as fractionating agents with optimal concentration (Deak, Murphy, 2006, 2007; Teng et al., 2009).

In addition, the change of $Ca(OH)_2$ and NaOH ratio modified the thermal behaviour of 7S and 11S differently. A stabilization of 7S and 11S (increase in T_d) in SPF was induced by the increase of the Ca content, but a lower Ca content is required to change the T_d of 11S than that of 7S. The T_d of 7S started to increase significantly when the Ca content changed from 6.47 to 9.84 mg/g protein (SPF 4 to SPF 5), while the T_d of 11S started to change when the Ca content was above 0.57 mg/g protein. Similar results were reported in the literature, where a Ca level above 5 mg/g in SPI was found to protect the soy proteins and partially prevent their denaturation (Scilingo & Añón, 1996). The addition of Ca ions in SPI dispersions produced higher T_d of both 7S and 11S, and

increased the enthalpy of denaturation, mainly the 11S fraction (Scilingo & Añón, 2004). These findings can be linked to the protein aggregation discussed above, and the cross-linking effects probably increase the thermal stability of the SPFs.

The viscosity of the SPF dispersions increased sharply when the Ca content in the SPF changed from 0.57 to 1.90 mg/g protein (SPF 1 to SPF 2) and reached a maximum. When the Ca content increased further, the viscosity of the mixture decreased. The viscosities of SPF 5, SPF 6, and SPF 7 measured at high shear rates were similar and much lower than SPF 4. These changes may be related to the soy protein-Ca complex formation. It was reported that Ca salt has been used as a thickening agent in soy protein suspensions (Lee & Rha, 1977). When Ca salts were added to the soy protein with low concentration without heating, the primary effect of Ca ions was likely to diminish repulsive forces. Protein: protein association occurred to form the matrix. By further Ca addition, the soluble soy proteins were bonded to a network and therefore, increased the viscosity. However, when the Ca content exceeded certain level, the effects of Ca bridges became dominate (Guo & Ono, 2005; Shun-Tang, Ono, & Mikami, 1999). The viscosity of high-Ca SPFs was close to the viscosity of water, which hinted that the larger aggregates induced by high-Ca content became denser and insoluble, and therefore, rarely interacted with water and contributed to the viscosity afterward. This hypothesis can be confirmed by the results of NSI and WHC_P. With the presence of higher Ca content, the decrease of NSI and WHC_P values indicated that the insoluble aggregations had limited ability to hold water, which means the volume of the aqueous phase was not highly influenced. As a result, the viscosity of SPF 5, SPF 6, and SPF 7 was much lower than the other SPFs.

The gelation ability of soy proteins is important for the textural properties of food systems. Soybean proteins can form heat-induced and cold-set gels (Zheng et al., 2019). Generally, G'' is greater than G' when a gel network structure is not formed, while when G' is greater than G'', this suggests that a gel network structure has formed. For SPF 1, SPF 2, SPF 3, and SPF 4, the G' and G'' declined as the temperature rose during the initial stage of heating (Fig. 9). As heating continued, a rapid increase of G' and G'' was observed, which originates mainly from protein denaturation and network formation. Similar gelation curves were also observed from SPI upon the heating (X. Li et al., 2020). The gelation temperature (T_{gel}) was around 65.54 °C for SPF 1, and increased to around 94.93 °C for SPF 3. This trend was in line with the uptrend of T_d for the SPFs (Table 3). However, the T_{gel} of SPF 4 and SPF 5 was dropped to 80.33 °C and 40.22 °C, respectively. This result can be linked to the PSD of the SPF dispersions (Fig. 4). The PSD of SPF 1, SPF 2, and SPF 3 was similar and single-peaked, while for SPF 4 and SPF 5, the PSD became wider towards the right side, which probably indicates rearrangements of Ca bridges and the formation of larger aggregations. An earlier study reported that the soybean protein aggregation promoted by Ca allows the gelation of proteins that were less denatured (Speroni, Añón, & de Lamballerie, 2010). For SPF 6 and SPF 7, the G' was higher than G'' even without heating. This means the gels were formed under room temperature, suggesting the formation of Ca-induced cold-set gels. Previous research reported that a cold-set gel of soy protein can be formed depending on the protein concentrations and $CaCl_2$ level (Maltais, Remondetto, Gonzalez, & Subirade, 2005). In the presence of a certain amount of Ca, the additional cross-linking could promote the formation of salt bridges between protein aggregates, allowing them to form a space-filling network at an early stage of protein unfolding (Lu, Lu, Yin, Cheng, & Li, 2010).

Even though SPFs with relatively high Ca content (SPF 4 to SPF 7) can form gels at lower or even at room temperature, the LVE regime of the corresponding gels was shorter with the increase of the Ca content, which means that the gel broke at smaller deformation. The results of PSD, NSI, and WHC_P (Figs. 4, 6 and 7) suggested that the larger Ca-induced aggregates were quite dense and inert, which could lead to the reduction of gel strength. Additionally, the lower net charge of SPFs with higher Ca content may shield electrostatic interactions at pH 7 between protein aggregates (Fig. 5), resulting in a weaker gel network. Other researchers also reported that the addition of Ca softened the gel strength of soy milk yogurt (Yazici, Alvarez, & Hansen, 1997).

5. Conclusion

In this study, a simplified fractionation process was employed using different alkali solutions with ranging NaOH and $Ca(OH)_2$ contents in the neutralization step. SPFs were produced with around 75%wt protein and increased Ca and reduced Na content at different levels. Ca enrichment gradually promoted the formation of larger particles, increased the thermal stability, reduced the NSI, WHC_P values, and changed the gelation properties of the SPFs. These effects were highly dependent on the Ca content in the SPFs. Although the morphology and functionalities of SPFs varied greatly at a high Ca level, at a lower Ca enrichment (<6.5 mg/g protein) they were affected to a limited extent. This indicated that a critical Ca and Na level can be achieved for simply fractionated soy protein without causing profound changes in its conformation and functional properties. Thus, Ca enrichment during the fractionation process can provide the possibility to increase the Ca content and reduce Na content of soy protein ingredients without compromising their use for novel soy-based foods. Future research could investigate the Ca bioavailability of soy protein ingredients, and how this would be affected by the use of different types of Ca salts.

Author statement

Yu Peng: Conceptualization, Methodology, Formal analysis, Investigation, Data curation, Visualization, Validation, Writing – original draft, Konstantina Kyriakopoulou: Conceptualization, Validation, Writing – review & editing, Supervision, Julia K. Keppler: Methodology, Data curation, Validation, Writing – review & editing, Paul Venema: Methodology & Validation, Atze Jan van der Goot: Conceptualization, Writing – review & editing, Supervision.

Declaration of competing interest

None.

Acknowledgements

The authors would like to thank the China Scholarship Council (CSC) and Plant Meat Matters project for financial support. The Plant Meat Matters project is co-financed by the Top Consortium for Knowledge and Innovation Agri & Food by the Dutch Ministry of Economic Affairs; the project is registered under contract number TKI-AF-16011.

Appendix A. Supplementary data

Supplementary data to this article can be found online at https://doi.org/10.1016/j.foodhyd.2021.107191.

References

Acosta, N. B., Sihufe, G. A., Meza, B. E., Marino, F., Costabel, L. M., Zorrilla, S. E., et al. (2020). Milk fortified with calcium: Changes in the physicochemical and rheological characteristics that affect the stability. *Lebensmittel-Wissenschaft & Technologie, 134*, 110204. https://doi.org/10.1016/j.lwt.2020.110204

Alhazmi, H. A. (2019). FT-IR spectroscopy for the identification of binding sites and measurements of the binding interactions of important metal ions with bovine serum albumin. *Scientia Pharmaceutica, 87*(1), 5. https://doi.org/10.3390/scipharm87010005

Appleby, P., Roddam, A., Allen, N., & Key, T. (2007). Comparative fracture risk in vegetarians and nonvegetarians in EPIC-Oxford. *European Journal of Clinical Nutrition, 61*(12), 1400–1406. https://doi.org/10.1038/sj.ejcn.1602659

Appurao, A. G., & R, M. N. (1975). Binding of Ca (II) by the 11S fraction of soybean proteins. *Cereal Chemistry, 52*, 21–23.

Baldassarre, M. E., Panza, R., Farella, I., Posa, D., Capozza, M., & Mauro, A. Di (2020). Vegetarian and vegan weaning of the infant: How common and how evidence-based?

A population-based survey and narrative review. *International Journal of Environmental Research and Public Health, 17*(13), 4835. https://doi.org/10.3390/ijerph17134835

Bhatia, J., & Greer, F. (2008). Use of soy protein-based formulas in infant feeding. https://doi.org/10.1542/peds.2008-0564.

Cobb, J. S., Zai-Rose, V., Correia, J. J., & Janorkar, A. V. (2020). FT-IR spectroscopic analysis of the secondary structures present during the desiccation induced aggregation of elastin-like polypeptide on silica. *ACS Omega, 5*(14), 8403–8413. https://doi.org/10.1021/acsomega.0c00271

Davey, G. K., Spencer, E. A., Appleby, P. N., Allen, N. E., Knox, K. H., & Key, T. J. (2003). EPIC–Oxford:lifestyle characteristics and nutrient intakes in a cohort of 33 883 meat-eaters and 31 546 non meat-eaters in the UK. *Public Health Nutrition, 6*(3), 259–268. https://doi.org/10.1079/phn2002430

Deak, N. A., & Johnson, L. A. (2007). Effects of extraction temperature and preservation method on functionality of soy protein. *JAOCS, Journal of the American Oil Chemists' Society, 84*(3), 259–268. https://doi.org/10.1007/s11746-007-1035-7

Deak, N. A., Murphy, P. A., & Johnson, L. A. (2006). Effects of NaCl concentration on salting-in and dilution during salting-out on soy protein fractionation. *Journal of Food Science, 71*(4). https://doi.org/10.1111/j.1750-3841.2006.00028.x

Deak, N. A., Murphy, P. A., & Johnson, L. A. (2007). Characterization of fractionated soy proteins produced by a new simplified procedure. *JAOCS, Journal of the American Oil Chemists' Society, 84*(2), 137–149. https://doi.org/10.1007/s11746-006-1017-1

Gaucheron, F. (2005, July 1). *The minerals of milk. Reproduction Nutrition Development*. EDP Sciences. https://doi.org/10.1051/rnd:2005030

Geerts, M. E. J., Dekkers, B. L., van der Padt, A., & van der Goot, A. J. (2018). Aqueous fractionation processes of soy protein for fibrous structure formation. *Innovative Food Science & Emerging Technologies, 45*, 313–319. https://doi.org/10.1016/J.IFSET.2017.12.002

Guo, S. T., & Ono, T. (2005). The role of composition and content of protein particles in soymilk on tofu curding by glucono-δ-lactone or calcium sulfate. *Journal of Food Science, 70*(4), C258–C262. https://doi.org/10.1111/j.1365-2621.2005.tb07170.x

Hoffman, J. R., & Falvo, M. J. (2004). Protein - which is best? Journal of sports science and medicine. Las. Retrieved from http://www.jssm.org.

Hongsprabhas, P., & Barbut, S. (1997). Structure-forming processes in Ca2+-induced whey protein isolate cold gelation. *International Dairy Journal, 7*(12), 827–834. https://doi.org/10.1016/S0958-6946(98)00011-9

Hu, H., Wu, J., Li-Chan, E. C. Y., Zhu, L., Zhang, F., Xu, X., et al. (2013). Effects of ultrasound on structural and physical properties of soy protein isolate (SPI) dispersions. *Food Hydrocolloids, 30*(2), 647–655. https://doi.org/10.1016/j.foodhyd.2012.08.001

Institute of Medicine (US). (2011). *Dietary reference intakes for calcium and vitamin D*. National Academies Press. https://doi.org/10.17226/13050

Itoh, R., & Suyama, Y. (1996). Sodium excretion in relation to calcium and hydroxyproline excretion in a healthy Japanese population. *American Journal of Clinical Nutrition*. https://doi.org/10.1093/ajcn/63.5.735

Jaramillo, D. P., Roberts, R. F., & Coupland, J. N. (2011). Effect of pH on the properties of soy protein-pectin complexes. *Food Research International, 44*(4), 911–916. https://doi.org/10.1016/j.foodres.2011.01.057

Kao, F. J., Su, N. W., & Lee, M. H. (2003). Effect of calcium sulfate concentration in soymilk on the microstructure of firm tofu and the protein constitutions in tofu whey. *Journal of Agricultural and Food Chemistry, 51*(21), 6211–6216. https://doi.org/10.1021/jf0342021

Kayser, J. J., Arnold, P., Steffen-Heins, A., Schwarz, K., & Keppler, J. K. (2020). Functional ethanol-induced fibrils: Influence of solvents and temperature on amyloid-like aggregation of beta-lactoglobulin. *Journal of Food Engineering, 270*, 109764. https://doi.org/10.1016/j.jfoodeng.2019.109764

Keller, J. L., Lanou, A. J., & Barnard, N. D. (2002). The consumer cost of calcium from food and supplements. *Journal of the American Dietetic Association, 102*(11), 1669–1671. https://doi.org/10.1016/S0002-8223(02)90355-X

Kneifel, W., Paquin, P., Abert, T., & Richard, J. P. (1991). Water-holding capacity of proteins with special regard to milk proteins and methodological aspects—a review. *Journal of Dairy Science, 74*(7), 2027–2041. https://doi.org/10.3168/JDS.S0022-0302(91)78373-2

Kong, J., & Yu, S. (2007). Fourier transform infrared spectroscopic analysis of protein secondary structures. *Acta Biochimica et Biophysica Sinica, 39*(8), 549–559. https://doi.org/10.1111/j.1745-7270.2007.00320.x

Kroll, R. D. (1984). Effect of pH on the binding of calcium ions by soybean proteins. *Cereal Chemistry*.

Krul, E. S. (2019). Calculation of nitrogen-to-protein conversion factors: A review with a focus on soy protein. *Journal of the American Oil Chemists' Society, 96*(4), 339–364. https://doi.org/10.1002/aocs.12196

Larsson, C. L., & Johansson, G. K. (2002). Dietary intake and nutritional status of young vegans and omnivores in Sweden. *American Journal of Clinical Nutrition*. https://doi.org/10.1093/ajcn/76.1.100

Lee, C. H., & Rha, C. (1977). Thickening of soy protein suspensions with calcium. *Journul of Texture Studies, 7*(3023), 441–449. https://doi.org/10.1111/j.1745-4603.1977.tb01151.x

Lee, C. H., & Rha, C. (1978). Microstructure OF soybean protein aggregates and its relation to the physical and textural properties OF the curd. *Journal of Food Science, 43*(1), 79–84. https://doi.org/10.1111/j.1365-2621.1978.tb09740.x

Li, X., Chen, L., Hua, Y., Chen, Y., Kong, X., & Zhang, C. (2020). Effect of preheating-induced denaturation during protein production on the structure and gelling properties of soybean proteins. *Food Hydrocolloids, 105*, 105846. https://doi.org/10.1016/j.foodhyd.2020.105846

Li, Z.-G., Yue, X.-Y., Liu, Y.-J., & Zhang, Y.-X. (2011). Effect of calcium salts and tri-sodium citrate on certain properties of calcium-fortified soy milk. *African Journal of Biotechnology, 10*(52), 10698–10705. https://doi.org/10.5897/AJB10.2053

Long, G., Ji, Y., Pan, H., Sun, Z., Li, Y., & Qin, G. (2015). Characterization of thermal denaturation structure and morphology of soy glycinin by FTIR and SEM. *International Journal of Food Properties, 18*(4), 763–774. https://doi.org/10.1080/10942912.2014.908206

Lu, X., Lu, Z., Yin, L., Cheng, Y., & Li, L. (2010). Effect of preheating temperature and calcium ions on the properties of cold-set soybean protein gel. *Food Research International, 43*(6), 1673–1683. https://doi.org/10.1016/j.foodres.2010.05.011

Lynch, H., Johnston, C., & Wharton, C. (2018). Plant-based diets: Considerations for environmental impact, protein quality, and exercise performance. *Nutrients, 10*(12), 1–16. https://doi.org/10.3390/nu10121841

Malhotra, A., & Coupland, J. N. (2004). The effect of surfactants on the solubility, zeta potential, and viscosity of soy protein isolates. *Food Hydrocolloids, 18*(1), 101–108. https://doi.org/10.1016/S0268-005X(03)00047-X

Maltais, A., Remondetto, G. E., Gonzalez, R., & Subirade, M. (2005). Formation of soy protein isolate cold-set gels: Protein and salt effects. *Journal of Food Science, 70*(1), C67–C73. https://doi.org/10.1111/j.1365-2621.2005.tb09023.x

Manassero, C. A., Vaudagna, S. R., Añón, M. C., & Speroni, F. (2015). High hydrostatic pressure improves protein solubility and dispersion stability of mineral-added soybean protein isolate. *Food Hydrocolloids, 43*, 629–635. https://doi.org/10.1016/j.foodhyd.2014.07.020

Matkovic, V., Ilich, J. Z., Andon, M. B., Hsieh, L. C., Tzagournis, M. A., Lagger, B. J., et al. (1995). Urinary calcium, sodium, and bone mass of young females. *American Journal of Clinical Nutrition*. https://doi.org/10.1093/ajcn/62.2.417

Mitchell, H. L. (2019). Alternative ingredients to sodium chloride. *Reducing Salt in Foods*, 113–128. https://doi.org/10.1016/B978-0-08-100890-4.00005-6

Mitsuda, H., Kusano, T., & Hasegawa, K. (1965). Purification of the 11 S component of soybean proteins. *Agricultural & Biological Chemistry, 29*(1), 7–12. https://doi.org/10.1271/bbb1961.29.7

Mulvihill, D. M., & Kinsella, J. E. (1988). Gelation of β-lactoglobulin: Effects of sodium chloride and calcium chloride on the rheological and structural properties of gels. *Journal of Food Science, 53*(1), 231–236. https://doi.org/10.1111/j.1365-2621.1988.tb10216.x

Nagano, T., Mori, H., & Nishinari, K. (1994). Rheological properties and conformational states of β-conglycinin gels at acidic pH. *Biopolymers, 34*(2), 293–298. https://doi.org/10.1002/bip.360340215

Peng, Y., Dewi, D. P. A. P., Kyriakopoulou, K., & van der Goot, A. J. (2020). *Effect of calcium hydroxide and fractionation process on the functional properties of soy protein concentrate*. Innovative Food Science & Emerging Technologies. https://doi.org/10.1016/j.ifset.2020.102501

Peng, Y., Kersten, N., Kyriakopoulou, K., & van der Goot, A. J. (2020). Functional properties of mildly fractionated soy protein as influenced by the processing pH. *Journal of Food Engineering, 275*, 109875. https://doi.org/10.1016/j.jfoodeng.2019.109875

Peters, J. P. C. M., Luyten, H., Alting, A. C., Boom, R. M., & Van der Goot, A. J. (2015). Effect of crosslink density on the water-binding capacity of whey protein microparticles. *Food Hydrocolloids, 44*, 277–284. https://doi.org/10.1016/j.foodhyd.2014.09.030

Peters, J. P. C. M., Vergeldt, F. J., Boom, R. M., & van der Goot, A. J. (2017). Water-binding capacity of protein-rich particles and their pellets. *Food Hydrocolloids, 65*, 144–156. https://doi.org/10.1016/j.foodhyd.2016.11.015

Piccini, L., Scilingo, A., & Speroni, F. (2019). Thermal versus high hydrostatic pressure treatments on calcium-added soybean proteins. Protein solubility, colloidal stability and cold-set gelation. *Food Biophysics, 14*(1), 69–79. https://doi.org/10.1007/s11483-018-9558-z

Preece, K. E. E., Hooshyar, N., & Zuidam, N. J. J. (2017). Whole soybean protein extraction processes: A review. *Innovative Food Science & Emerging Technologies, 43* (July), 163–172. https://doi.org/10.1016/j.ifset.2017.07.024

Rekha, C. R., & Vijayalakshmi, G. (2013). Influence of processing parameters on the quality of soycurd (tofu). *Journal of Food Science & Technology, 50*(1), 176–180. https://doi.org/10.1007/s13197-011-0245-z

Rizzo, G., & Baroni, L. (2018). *Soy, soy foods and their role in vegetarian diets. Nutrients* (Vol. 10). MDPI AG. https://doi.org/10.3390/nu10010043

Sakakibara, M., & Noguchi, H. (1977). Interaction of lis fraction of soybean protein with calcium ion. *Agricultural & Biological Chemistry, 41*(9), 1575–1580. https://doi.org/10.1080/00021369.1977.10862744

Scilingo, A. A., & Añón, M. C. (1996). Calorimetric study of soybean protein isolates: Effect of calcium and thermal treatments. *Journal of Agricultural and Food Chemistry, 44*(12), 3751–3756. https://doi.org/10.1021/jf960035b

Scilingo, A. A., & Añón, M. C. (2004). Characterization of soybean protein isolates. The effect of calcium presence. *JAOCS, Journal of the American Oil Chemists' Society, 81* (1), 63–69. https://doi.org/10.1007/s11746-004-0858-y

Shun-Tang, G., Ono, T., & Mikami, M. (1999). Incorporation of soy milk lipid into protein coagulum by addition of calcium chloride. *Journal of Agricultural and Food Chemistry, 47*(3), 901–905. https://doi.org/10.1021/jf9805247

Song, X., Zhou, C., Fu, F., Chen, Z., & Wu, Q. (2013). Effect of high-pressure homogenization on particle size and film properties of soy protein isolate. *Industrial Crops and Products, 43*(1), 538–544. https://doi.org/10.1016/j.indcrop.2012.08.005

Speroni, F., Añón, M. C., & de Lamballerie, M. (2010). Effects of calcium and high pressure on soybean proteins: A calorimetric study. *Food Research International, 43* (5), 1347–1355. https://doi.org/10.1016/j.foodres.2010.03.022

Spotti, M. J., Tarhan, Ö., Schaffter, S., Corvalan, C., & Campanella, O. H. (2017). Whey protein gelation induced by enzymatic hydrolysis and heat treatment: Comparison of

creep and recovery behavior. *Food Hydrocolloids, 63*, 696–704. https://doi.org/10.1016/j.foodhyd.2016.10.014

Strazzullo, P., D'Elia, L., Kandala, N. B., & Cappuccio, F. P. (2009). Salt intake, stroke, and cardiovascular disease: Meta-analysis of prospective studies. *BMJ*. https://doi.org/10.1136/bmj.b4567 (online).

Teng, Z., Liu, C., Yang, X., Li, L., Tang, C., & Jiang, Y. (2009). Fractionation of soybean globulins using Ca2+ and Mg 2+: A comparative analysis. *JAOCS, Journal of the American Oil Chemists' Society, 86*(5), 409–417. https://doi.org/10.1007/s11746-009-1367-6

Thrane, M., Paulsen, P. V., Orcutt, M. W., & Krieger, T. M. (2017). Soy protein: Impacts, production, and applications. In *Sustainable protein sources* (pp. 23–45). Elsevier Inc. https://doi.org/10.1016/B978-0-12-802778-3.00002-0.

Tuso, P. J., Ismail, M. H., Ha, B. P., & Bartolotto, C. (2013). Nutritional update for physicians: Plant-based diets. *The Permanente Journal, 17*(2), 61–66. https://doi.org/10.7812/TPP/12-085

Weaver, C. M., Heaney, R. P., Connor, L., Martin, B. R., Smith, D. L., & Nielsen, S. (2002). Bioavailability of calcium from tofu as compared with milk in premenopausal women. *Journal of Food Science, 67*(8), 3144–3147. https://doi.org/10.1111/j.1365-2621.2002.tb08873.x

Weaver, C. M., Heaney, R. P., Proulx, W. R., Hinders, S., & Packard, P. T. (1993). Absorbability of calcium from common beans. *Journal of Food Science, 58*(6), 1401–1403. https://doi.org/10.1111/j.1365-2621.1993.tb06192.x

Wójcik, P., Rogowska, M., Chyćko, M., Tomczyk, J., Sobstyl, A., Krasowska, D., et al. (2020). Influence of vegetarian diet on human body. *Journal of Education, Health and Sport, 10*(9), 739. https://doi.org/10.12775/jehs.2020.10.09.089

Yazici, F., Alvarez, V. B., & Hansen, P. M. T. (1997). Fermentation and properties of calcium-fortified soy milk yogurt. *Journal of Food Science, 62*(3), 457–461. https://doi.org/10.1111/j.1365-2621.1997.tb04406.x

Yazici, F., Alvarez, V. B., Mangino, M. E., & Hansen, P. M. T. (1997). Formulation and processing of a heat stable calcium-fortified soy milk. *Journal of Food Science, 62*(3), 535–538. https://doi.org/10.1111/j.1365-2621.1997.tb04424.x

Yuan, Y. J., Velev, O. D., Chen, K., Campbell, B. E., Kaler, E. W., & Lenhoff, A. M. (2002). Effect of pH and Ca2+-induced associations of soybean proteins. *Journal of Agricultural and Food Chemistry, 50*(17), 4953–4958. https://doi.org/10.1021/jf025582d

Zayas, J. F. (1997). Water holding capacity of proteins. *Functionality of Proteins in Food*, 76–133. https://doi.org/10.1007/978-3-642-59116-7_3

Zhang, J., Liang, L., Tian, Z., Chen, L., & Subirade, M. (2012). Preparation and in vitro evaluation of calcium-induced soy protein isolate nanoparticles and their formation mechanism study. *Food Chemistry, 133*(2), 390–399. https://doi.org/10.1016/j.foodchem.2012.01.049

Zhao, X., Chen, F., Xue, W., & Lee, L. (2008). FTIR spectra studies on the secondary structures of 7S and 11S globulins from soybean proteins using AOT reverse micellar extraction. *Food Hydrocolloids, 22*(4), 568–575. https://doi.org/10.1016/j.foodhyd.2007.01.019

Zhao, Y., Martin, B. R., & Weaver, C. M. (2005). Calcium bioavailability of calcium carbonate fortified soymilk is equivalent to cow's milk in young women. *Journal of Nutrition, 135*, 2379–2382. https://doi.org/10.1093/jn/135.10.2379. American Institute of Nutrition.

Zheng, L., Teng, F., Wang, N., Zhang, X.-N., Regenstein, J., Liu, J.-S., et al. (2019). Addition of salt ions before spraying improves heat- and cold-induced gel properties of soy protein isolate (SPI). *Applied Sciences, 9*(6), 1076. https://doi.org/10.3390/app9061076